

Supporting Information

Photoactivatable BODIPYs Designed to Monitor the Dynamics of Supramolecular Nanocarriers

Yang Zhang,[†] Subramani Swaminathan,[†] Sicheng Tang,[†] Jaume Garcia-Amorós,[†] Marcia Boulina,[‡] Burjor Captain,[†] James D. Baker[§] and
Francisco M. Raymo^{*,†}

Laboratory for Molecular Photonics, Department of Chemistry, University of Miami, 1301 Memorial Drive, Coral Gables, FL 33146-0431, Department of Biology, University of Miami, 1301 Memorial Drive, Coral Gables, FL 33146-0431 and Analytical Imaging Core Facility, Diabetes Research Institute, University of Miami, 1450 NW 10th Avenue, Miami, FL 33136

E-Mail: fraymo@miami.edu

• Crystallographic Data for 1	S2
• Emission Spectra of 2 , 3 , 5 , 6 and 12	S3
• Differential Pulse Voltammograms of 1 and 12	S3
• Dependence of the Emission Intensity of 12 on the Concentration of 13	S3
• Fluorescence Images of 3 in PBMA	S4
• Fluorescence Images of Nanoparticles of 13 , Doped with 3 or 12 , in Alginate Hydrogels	S4
• Fluorescence Images of Nanoparticles of 13 , Doped with 3 , in <i>Drosophila Melanogaster</i> Embryos	S5

[†] Department of Chemistry

[‡] Diabetes Research Institute

[§] Department of Biology

Table S1. Crystallographic Data for **1**.

<i>Empirical Formula</i>	C ₁₈ H ₁₈ N ₂ O ₃
<i>Formula Weight</i>	310.34
<i>Crystal System</i>	Monoclinic
<i>Lattice Parameters:</i>	
<i>a</i> (Å)	8.2502(3)
<i>b</i> (Å)	17.5045(6)
<i>c</i> (Å)	11.1549(4)
<i>β</i> (°)	105.933(1)
<i>V</i> (Å ³)	1549.05(10)
<i>Space Group</i>	<i>P</i> 2 ₁ / <i>n</i> (# 14)
<i>Z</i> Value	4
<i>ρ</i> _{calc} (g cm ⁻³)	1.331
<i>μ</i> (Mo Kα) (mm ⁻¹)	0.092
<i>T</i> (K)	296
<i>2Θ</i> _{max} (°)	54.0
<i>No. Obs.</i> (<i>I</i> > 2σ(<i>I</i>))	3046
<i>No. Parameters</i>	212
<i>Goodness of Fit</i>	1.043
<i>Max. Shift in Cycle</i>	0.001
<i>Residuals</i> *: R1; wR2	0.0392; 0.1063
<i>Absorption Correction</i> ,	Multi-scan
<i>Max/min</i>	0.9819/0.9556
<i>Largest Peak in Final Diff. Map</i> (e ⁻ Å ⁻³)	0.201

$$* \text{ R} = \sum_{\text{hkl}} (|F_{\text{obs}}| - |F_{\text{calc}}|) / \sum_{\text{hkl}} |F_{\text{obs}}|; \text{ R}_w = [\sum_{\text{hkl}} w(|F_{\text{obs}}| - |F_{\text{calc}}|)^2 / \sum_{\text{hkl}} w F_{\text{obs}}^2]^{1/2},$$

$$w = 1/\sigma^2(F_{\text{obs}}); \text{ GOF} = [\sum_{\text{hkl}} w(|F_{\text{obs}}| - |F_{\text{calc}}|)^2 / (n_{\text{data}} - n_{\text{vari}})]^{1/2}.$$

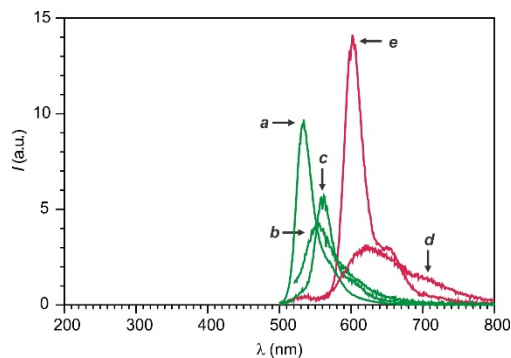


Figure S1. Emission spectra (10 μ M, MeCN, 25 $^{\circ}$ C, λ_{Ex} for **2**, **3**, **6** and **12** = 480 nm, λ_{Ex} for **5** = 540 nm) of **12** (*a*), **2** (*b*), **3** (*c*), **5** (*d*) and **6** (*e*).

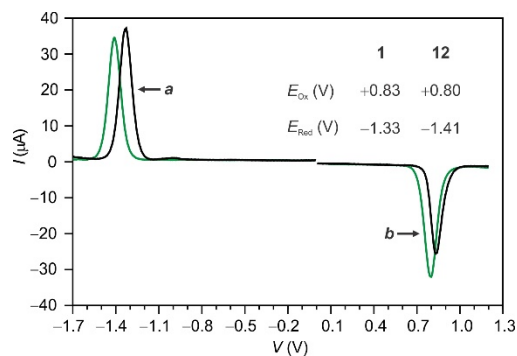


Figure S2. Differential pulse voltammograms [1 mM, MeCN, Bu_4NPF_6 (0.1 M), V vs. Ag/AgCl, 50 mV s^{-1} , 50 mV] of **1** (*a*) and **12** (*b*).

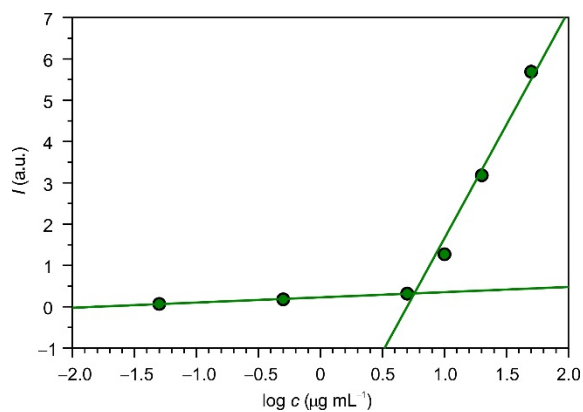


Figure S3. Plot of the emission intensity of **12** (5 $\mu\text{g mL}^{-1}$, λ_{Ex} = 470 nm, λ_{Em} = 536 nm) against the concentration of **13** in PBS at 25 $^{\circ}$ C.

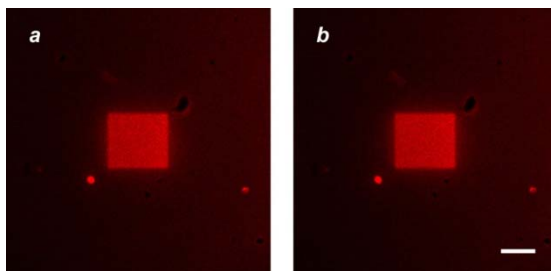


Figure S4. Fluorescence images (scale bar = 100 μm) of a PBMA film, doped with **3** (0.25% w/w), recorded with a λ_{Ex} of 594 nm and a detection window of 610–700 nm 5 (*a*) and 10 min (*b*) after activation of a rectangular region at a λ_{Ac} of 405 nm.

Web Enhanced Object

Video S1. Sequence of 43 fluorescence images of an alginate hydrogel, doped with nanoparticles of **13** ($250 \mu\text{g mL}^{-1}$) containing **3** ($2.5 \mu\text{g mL}^{-1}$), recorded with a λ_{Ex} of 594 nm, a detection window of 610–700 nm and a delay between frames of 15 s after activation of a rectangular region at a λ_{Ac} of 405 nm for 10 s.

Web Enhanced Object

Video S2. Sequence of 15 fluorescence images of an alginate hydrogel, doped with nanoparticles of **13** ($250 \mu\text{g mL}^{-1}$) containing **12** ($2.5 \mu\text{g mL}^{-1}$), recorded with a λ_{Ex} of 514 nm, a detection window of 530–650 nm and a delay between frames of 15 s after bleaching of a rectangular region at 405 nm for 60 s.

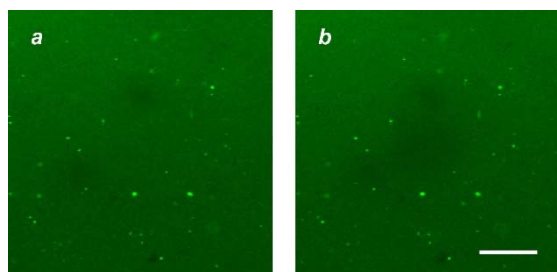


Figure S5. Fluorescence images (scale bar = 50 μm) of an alginate hydrogel, doped with nanoparticles of **13** ($250 \mu\text{g mL}^{-1}$) containing **12** ($2.5 \mu\text{g mL}^{-1}$), recorded with a λ_{Ex} of 514 nm and a detection window of 530–650 nm before (*a*) and after (*b*) bleaching of a rectangular region at 405 nm for 10 s.

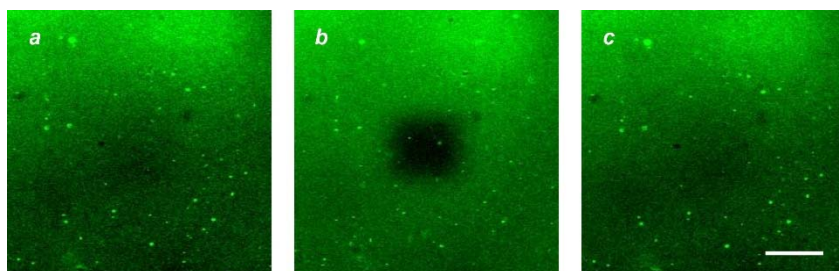


Figure S6. Fluorescence images (scale bar = 50 μm) of an alginate hydrogel, doped with nanoparticles of **13** ($250 \mu\text{g mL}^{-1}$) containing **12** ($2.5 \mu\text{g mL}^{-1}$), recorded with a λ_{Ex} of 514 nm and a detection window of 530–650 nm before (*a*) and after (*b*) bleaching of a rectangular region at 405 nm for 60 s and 210 s after bleaching (*c*).

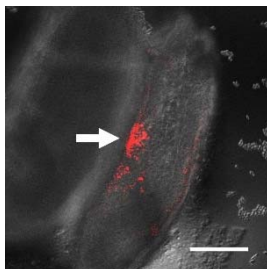


Figure S7. Overlaid fluorescence and transmittance images (scale bar = 100 μm) of two adjacent *Drosophila Melanogaster* embryos, one of which was microinjected with a solution of nanoparticles of **13** (5 mg mL^{-1}) containing **3** (50 $\mu\text{g mL}^{-1}$) in Dulbecco's PBS, recorded with a λ_{Ex} of 594 nm and a detection window of 610–700 nm 2250 s after activation of the indicated area at a λ_{Ac} of 405 nm for 10 s.

Web Enhanced Object

Video S3. Sequence of 15 overlaid fluorescence and transmittance images of two adjacent *Drosophila Melanogaster* embryos, one of which was microinjected with a solution of nanoparticles of **13** (5 mg mL^{-1}) containing **3** (50 $\mu\text{g mL}^{-1}$) in Dulbecco's PBS, recorded with a λ_{Ex} of 594 nm, a detection window of 610–700 nm and a delay between frames of 150 s after activation of a portion of the sample at a λ_{Ac} of 405 nm for 10 s.